Journal of Engineering Research

Volume 7
Issue 5 *This is a Special Issue from the Applied Innovative Research in Engineering Grand Challenges (AIRGEC) Conference, (AIRGEC 2023), Faculty of Engineering, Horus University, New Damietta, Egypt, 25-26 October 2023*

Article 24

2023

Modelling and simulation of drone's airfoil

Asmaa ElBahloul, Abdullah Elshenawy

Engineering Research Journal (ERJ)
Vol. 7 – No. 5, 2023
©Tanta University, Faculty of Engineering
ISSN: 2356-9441 https://erjeng.journals.ekb.eg/ e ISSN: 2735-4873

Modelling and simulation of drone's airfoil

Asmaa A. ElBahloul[1], Abdullah Elshennawy[2]

[1] Mechatronics Department, Faculty of Engineering, Horus University, New Damietta, Egypt – email: aelbahloul@horus.edu.eg
[2] Mechatronics Department, Faculty of Engineering, Horus University, New Damietta, Egypt – email: ashennawy@horus.edu.eg

***Abstract*- This paper proposes a different innovative design of airfoils used in drones. A computational fluid dynamic (CFD) model is built to model and simulate velocity and pressure profiles of the airfoil. Simulation is carried out by COMSOL Multiphysics. Airfoil design no. A is simulated at different normal inflow velocity. Resulted lift and drag forces are 12.04 N and 2.27 N at a normal inflow velocity of 7 m/s. For the simulation of different airfoil design thickness, airfoil no. B achieved a total lift force of 22.83 N and a total drag force of 1.29 N.**

***Keywords*- Drones, Airfoil, Drag force, Lift force, COMSOL.**

I. Introduction

Drones are a fast-evolving technology that are being used in many applications like military, public, industrial, and medical sectors. Drones are unmanned aerial vehicles (UAVs) which are aircrafts that can fly independently of being piloted by humans. It could be operated autonomously by onboard computers or remotely by a human operator [1]. During the projected time frame of 2021-2026, the drones market is anticipated to grow at a compound annual growth rate (CAGR) of 15.37% [2]. Therefore, improving the aerodynamics performance of drones become one of the most crucial concerns facing the aviation sector.

Drones wings are designed to achieve highest performance in altitude control, take-off, and landing [3]. Fixed-wing drones are attracting the attentions due to their low cruise-speed capabilities, short takeoff distance, and large payload, with high lift force producing abilities at low speed. Airfoil design affect the capability of fixed-wing drone to produce drag and lift forces [4]. The cross section of the wing is called airfoil. Airfoil significantly influences the creation of lift force by altering the rate of air passes over and beneath the surface of the wings [5].

The design of drone airfoil attracted the sight of researchers in the last few years. Chhari et al. [5], simulated different airfoil designs at drone speed15 m/s. Rajendran and Jayaprakash [6], modeled a proposed twin-blade propeller which achieved a torque of 1.1007 N.m and a peak coefficient of performance of 0.5810 at velocity of 15 m/s. Aminjan et al. [6], tested the performance of airfoil at an inlet angle of 0° and 30° and computed different drag and lift forces.

Tan et al. [7], simulated flight dynamics of a drone to asses noise of drone. They found that by reducing the drone flying speed and payload resulted in reducing the instantaneous noise of drone. Guo et al. [8], studied the hydrodynamic performance of airfoil in water. They achieved a maximum drag reduction of 25.4% at a velocity of 0.8 m/s.

Prieto et al. [9], carried out an optimization of a drone wing by using raked wingtips and blended winglets. Kumar et al. [10], reviewed recent progress conducted for underwater drones applications. Singh et al. [11], reviewed the classification of actuation mechanism designs for flapping-wing drones.

II. Theoretical Model

In this study, COMSOL Multiphysics is used to model the drone's airfoil [12]. The model assumptions are:

(i) steady state,
(ii) incompressible,
(iii) laminar,

to simplify the solution. In the developed model, sub-model interface is activated to simulate the airfoil. A schematic diagram of the two-dimension computational domain is depicted in Fig. 1 with a width of 2 m and height of 0.35 m.

A. Laminar Flow Interface

In the laminar flow interface, the velocity and pressure fields for the flow of a single-phase fluid in the laminar flow regime is computed. The equations solved by the Laminar Flow interface are the Navier-Stokes equations for conservation of momentum and the continuity equation for conservation of mass.

There are two main parameter that affects the performance of drone's airfoil model simulation. The first one is the drag force which is defined as the component of the resultant pressure and shear forces that acts in the flow direction [13]. Drag force (F_D)is defined as:

$$F_D = 0.5 C_D \rho V^2 A \quad (1)$$

where, F_D is the drag force (N)
C_D is the drag coefficient
ρ is the fluid's density (kg/m^3)
V is the drone's mean velocity (m/s)
A is the vertical projected area of airfoil (m^2)

And the component that acts normal to the flow direction is called the lift force [13]. Lift force (F_L) is defined as:

$$F_L = 0.5 C_L \rho V^2 A \quad (2)$$

where, F_D is the drag force (N)
C_D is the drag coefficient
A is the horizontal projected area of airfoil (m^2)

Air is used as fluid material The input data for laminar flow interface is shown in table 1. The mesh sequence was set as "physics-controlled mesh", and element size was set as "normal". The airfoil mesh distribution is shown in Fig. 2.

doi: 10.21608/erjeng.2023.238570.1262

Table 1: The input data for laminar flow interface

Parameter	Value
Air density (kg/m^3)	1.184
Air viscosity (Pa.s)	1.849*10^{-5}
Normal inflow velocity [m/s]	7

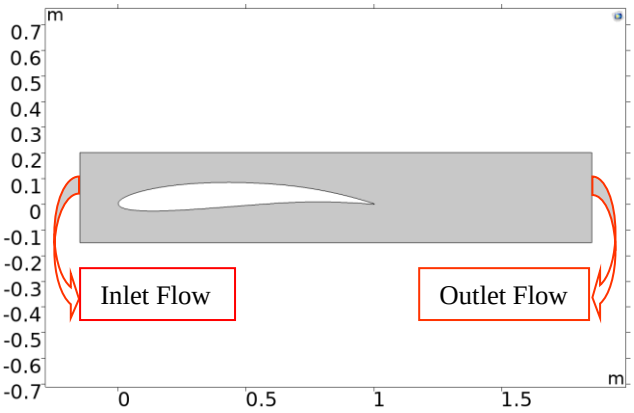

Fig. 1 Computational domain used to simulate the airfoil no. A

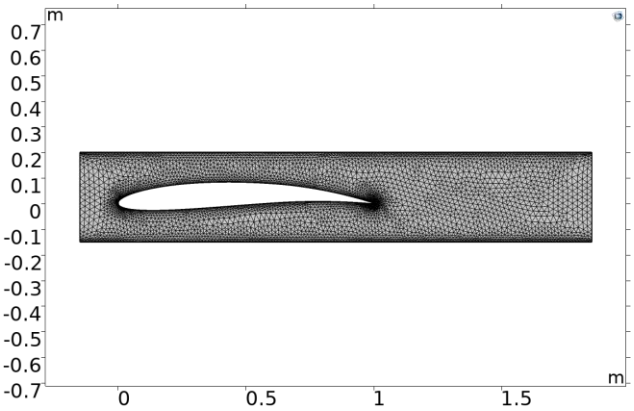

Fig. 2 The airfoil mesh distribution of airfoil no. A

III. Results and Discussion

This simulation investigation is carried out to show velocity and pressure profile for drone's airfoil. The results section starts by showing simulation investigation for airfoil no. A. Followed by the simulation investigation at different velocities. Then, a simulation investigation for different thickness of airfoil is conducted to compare between them.

A. Velocity And Pressure Profile for Airfoil No. A

For airfoil no. A, a CFD model is used to investigate the performance at a normal inflow velocity of 7 m/s with air as working fluid at atmospheric pressure. The resulted velocity and pressure profile for drone's airfoil are depicted in Fig. 3 and Fig. 4 respectively.

From Fig. 3, it can be seen that at the inlet tip of airfoil velocity decreases from normal inflow velocity until it reaches minimum value at the surface. Then increases at top side of airfoil. From Fig. 4, it can be seen that pressure increases at inlet tip of airfoil then decreases along bottom side. The effect of both velocity and pressure variation results in a total lift force of 12.04 N and a total drag force of 2.27 N.

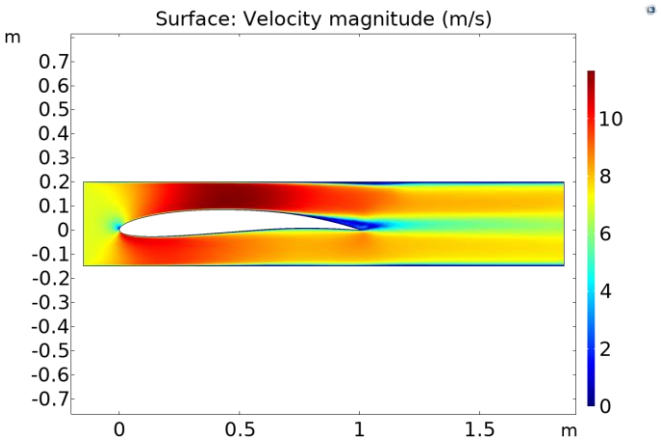

Fig. 3 Velocity profile of airfoil no. A at normal inflow velocity of 7 m/s

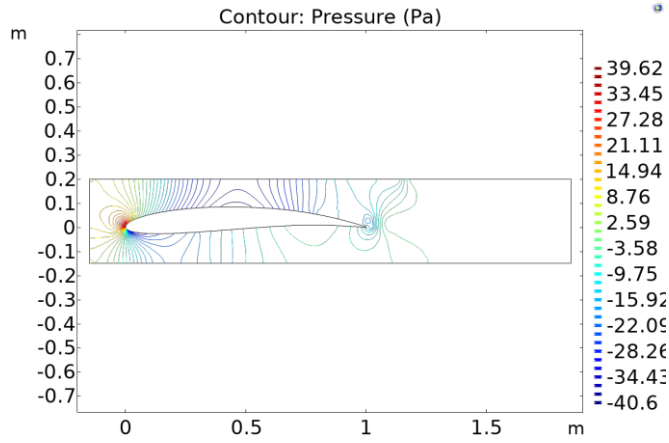

Fig. 4 Pressure profile of airfoil no. A at normal inflow velocity of 7 m/s

B. Velocity And Pressure Profile for Airfoil No. A At Different Velocity Inlet

For airfoil no. A, the CFD model is computed at different normal inflow velocity of 5 m/s and 9 m/s and their lift and drag forces are compared with the results at normal inflow velocity of 7 m/s. Air is the working fluid at atmospheric pressure. The resulted velocity and pressure profile for normal inflow velocity of 5 m/s are depicted in Fig. 5 and Fig. 6 respectively. And the resulted velocity and pressure profile for normal inflow velocity of 9 m/s are depicted in Fig. 7 and Fig. 8 respectively.

From Fig. 5, it can be seen that at the inlet tip of airfoil velocity decreases from normal inflow velocity until it reaches minimum value at the surface. Then increases at top side of airfoil. From Fig. 6, it can be seen that pressure increases at inlet tip of airfoil then decreases along bottom side. The effect of both velocity and pressure variation results in a total lift force of 5.09 N and a total drag force of 1.32 N.

From Fig. 7, it can be seen that at the inlet tip of airfoil velocity decreases from normal inflow velocity until it reaches minimum value at the surface. Then increases at top side of airfoil. From Fig. 8, it can be seen that pressure increases at inlet tip of airfoil then decreases along bottom

doi: 10.21608/erjeng.2023.238570.1262

side. The effect of both velocity and pressure variation results in a total lift force of 22.01 N and total drag force of 3.51 N.

Therefore, the total left forces and drag forces that affects the airfoil increases by increasing the normal inflow velocity.

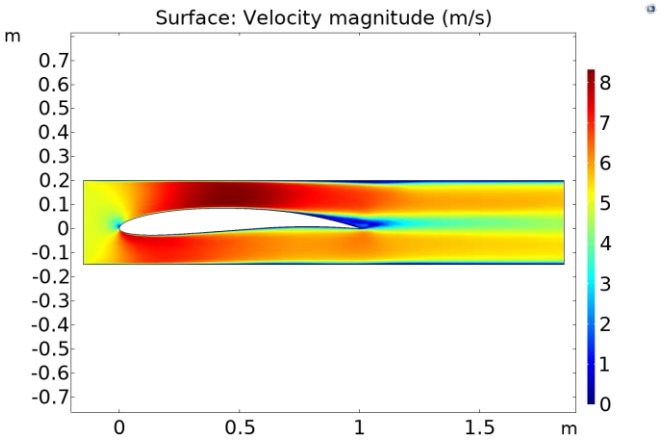

Fig. 5 Velocity profile of airfoil no. A at normal inflow velocity of 5 m/s

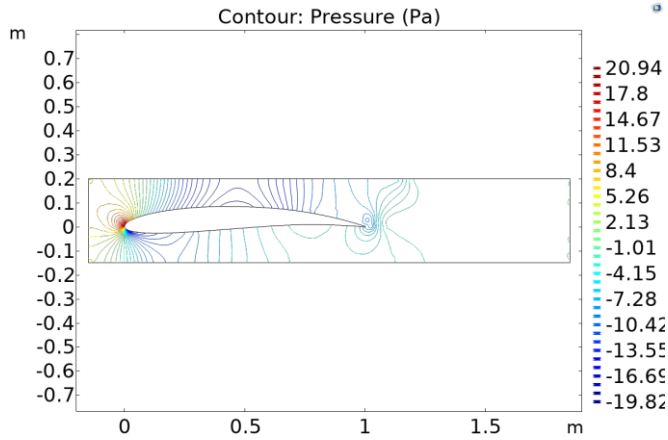

Fig. 6 Pressure profile of airfoil no. A at normal inflow velocity of 5 m/s

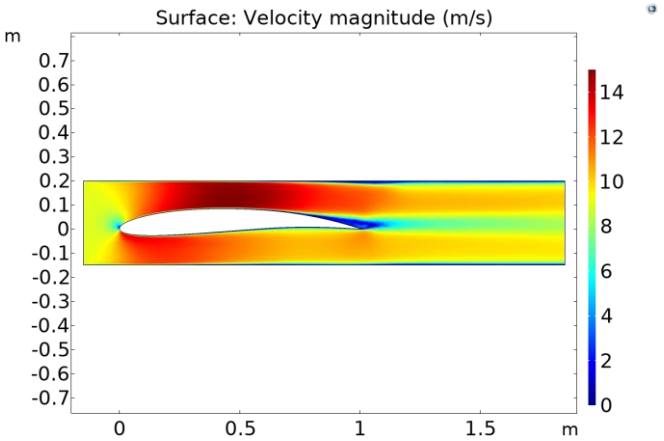

Fig. 7 Velocity profile of airfoil no. A at normal inflow velocity of 9 m/s

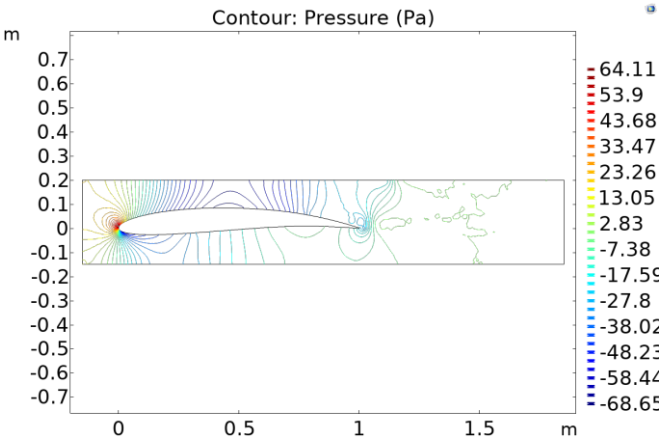

Fig. 8 Pressure profile of airfoil no. A at normal inflow velocity of 9 m/s

C. Comparison Between Different Airfoil Design Thickness

The following study is carried out to assess the performance of drone's airfoil at different airfoil thickness. Airfoil no. B thickness is lower than no. A by 5 %. And airfoil no. C thickness is higher than no. A by 5 %. The shape and computational domain of airfoil no. B and no. C is depicted in Fig. 9 and Fig. 10 respectively.

For airfoil no. B and C, a CFD model is used to investigate the performance at a normal inflow velocity of 7 m/s with air as working fluid at atmospheric pressure. The resulted velocity and pressure profile for drone's airfoil no. B are depicted in Fig. 11 and Fig. 12 respectively.

From Fig. 11 and Fig. 12, it can be seen that the difference between velocity and pressure at top surface and bottom surface is significant at no. B airfoil. The velocity is higher at the top surface and the pressure is higher at bottom surface. The effect of both velocity and pressure variation resulted in a total lift force of 22.83 N and a total drag force of 1.29 N. Therefore, the performance of airfoil no. B is much better than the performance of airfoil no. A.

The resulted velocity profile for drone's airfoil no. C is depicted in Fig. 13. From Fig. 13, it can be seen that the velocity on the top surface of airfoil is lower than that on the bottom surface. The effect of both velocity and pressure variation resulted in a negative total lift force of -9.60 N. this mean that the drone cannot fly with this airfoil design.

doi: 10.21608/erjeng.2023.238570.1262

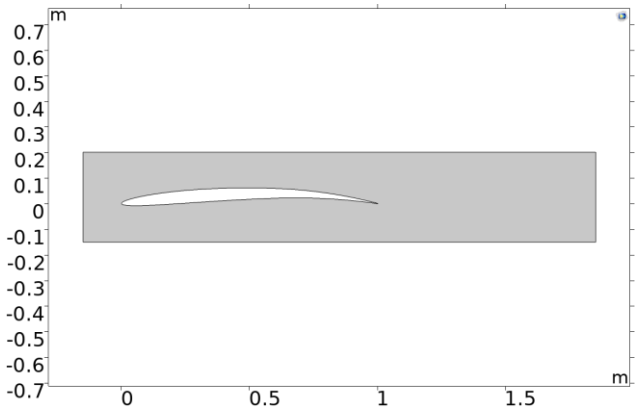

Fig. 9 Computational domain used to simulate the airfoil no. B

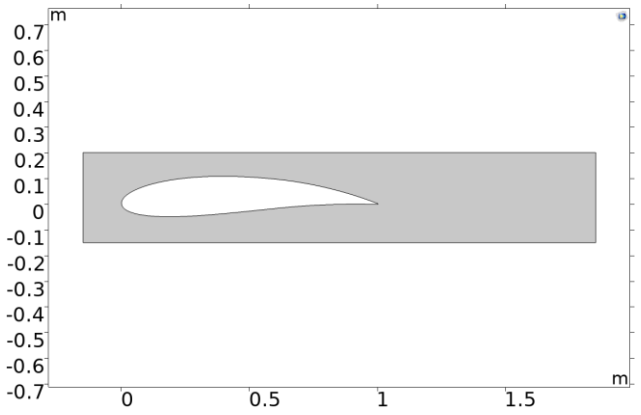

Fig. 10 Computational domain used to simulate the airfoil no. C

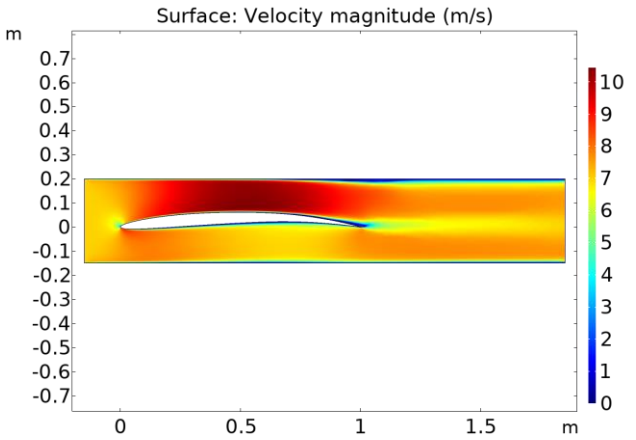

Fig. 11 Velocity profile of airfoil no. B at normal inflow velocity of 7 m/s

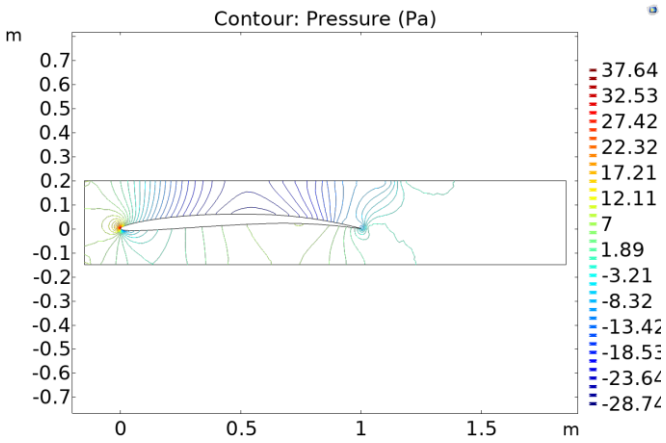

Fig. 12 Pressure profile of airfoil no. B at normal inflow velocity of 7 m/s

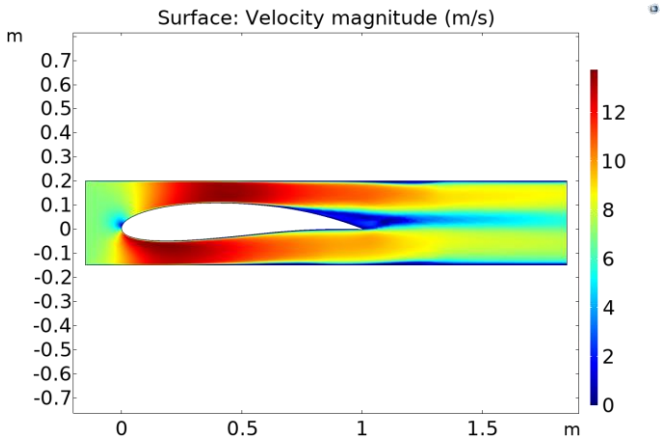

Fig. 13 Velocity profile of airfoil no. C at normal inflow velocity of 7 m/s

IV. Conclusion

In this study, a CFD model of drone airfoil is modeled and simulated at different normal inflow velocities and different airfoil thickness. The main outputs that have been concluded from this study are:

- The total left forces and drag forces that affects the airfoil increases by increasing the normal inflow velocity.
- For airfoil no. A, at a normal inflow velocity of 7 m/s a total lift force of 12.04 N and a total drag force of 2.27 N are achieved.
- And achieved a total lift force of 5.09 N and a total drag force of 1.32 N at a normal inflow velocity of 5 m/s.
- And achieved a total lift force of 22.01 N and total drag force of 3.51 N at normal inflow velocity of 9 m/s.
- For airfoil no. B, at a normal inflow velocity of 7 m/s a total lift force of 22.83 N and a total drag force of 1.29 N are achieved.
- The performance of airfoil no. B is much better than the performance of airfoil no. A.

doi: 10.21608/erjeng.2023.238570.1262

Journal of Engineering Research (ERJ)
Vol. 7 – No. 3, 2023
©Tanta University, Faculty of Engineering
ISSN: 2356-9441 https://erjeng.journals.ekb.eg/ e ISSN: 2735-4873

Conflicts of Interest: The authors declare that they have no known competing financial interests or personal relationships that could have appeared to influence the work reported in this paper.

REFERENCES

[1] N. Karpen, S. Diebald, F. Dezitter, and E. Bonaccurso, "Propeller-integrated airfoil heater system for small multirotor drones in icing environments: Anti-icing feasibility study," Cold Reg. Sci. Technol., vol. 201, p. 103616, 2022, doi: https://doi.org/10.1016/j.coldregions.2022.103616.

[2] T. Dbouk and D. Drikakis, "Computational aeroacoustics of quadcopter drones," Appl. Acoust., vol. 192, p. 108738, 2022, doi: https://doi.org/10.1016/j.apacoust.2022.108738.

[3] S. Du and H. Ang, "Design and Feasibility Analyses of Morphing Airfoil Used to Control Flight Attitude," Strojniški Vestn. - J. Mech. Eng., 2012, doi: 10.5545/sv-jme.2011.189.

[4] H. Zhu, H. Nie, L. Zhang, X. Wei, and M. Zhang, "Design and assessment of octocopter drones with improved aerodynamic efficiency and performance," Aerosp. Sci. Technol., vol. 106, p. 106206, 2020, doi: https://doi.org/10.1016/j.ast.2020.106206.

[5] K. Chhari, U. Raj, A. Galav, L. Dhillon, P. Tiwari, and J. Preet Singh, "Aerodynamic and bending analysis of low-speed airfoils at high reynold number," Mater. Today Proc., vol. 72, pp. 1524–1529, 2023, doi: https://doi.org/10.1016/j.matpr.2022.09.381.

[6] P. Rajendran and A. Jayaprakash, "Numerical performance analysis of a twin blade drone rotor propeller," Mater. Today Proc., vol. 80, pp. 492–498, 2023, doi: https://doi.org/10.1016/j.matpr.2022.10.201.

[7] Q. Tan et al., "Virtual flight simulation of delivery drone noise in the urban residential community," Transp. Res. Part D Transp. Environ., vol. 118, p. 103686, 2023, doi: https://doi.org/10.1016/j.trd.2023.103686.

[8] C. Guo, Y. Wu, Y. Han, and K. LingHu, "Experimental study on influence of sharkskin denticles structure on the hydrodynamic performance of airfoil," Ocean Eng., vol. 271, p. 113756, 2023, doi: https://doi.org/10.1016/j.oceaneng.2023.113756.

[9] M. Prieto, M. S. Escarti-Guillem, and S. Hoyas, "Aerodynamic optimization of a VTOL drone using winglets," Results Eng., vol. 17, p. 100855, 2023, doi: https://doi.org/10.1016/j.rineng.2022.100855.

[10] A. Kumar et al., "Blockchain for unmanned underwater drones: Research issues, challenges, trends and future directions," J. Netw. Comput. Appl., vol. 215, p. 103649, 2023, doi: https://doi.org/10.1016/j.jnca.2023.103649.

[11] S. Singh, M. Zuber, M. N. Hamidon, N. Mazlan, A. A. Basri, and K. A. Ahmad, "Classification of actuation mechanism designs with structural block diagrams for flapping-wing drones: A comprehensive review," Prog. Aerosp. Sci., vol. 132, p. 100833, 2022, doi: https://doi.org/10.1016/j.paerosci.2022.100833.

[12] "COMSOL Multiphysics® v. 5.6. COMSOL AB, Stockholm, Sweden. https://www.comsol.com/".

[13] A. Cengel Yunus, Fluid mechanics: Fundamentals and applications, 4th ed. Columbus, OH: McGraw-Hill Education, 2018.